IEEE Photonics Journal
An IEEE Photonics Society Publication

Open Access

Surface Plasmon Polaritons Propagation Through a Schottky Junction: Influence of The Inversion Layer

Volume 5, Number 2, April 2013

T. M. Wijesinghe, Member, IEEE
M. Premaratne, Senior Member, IEEE

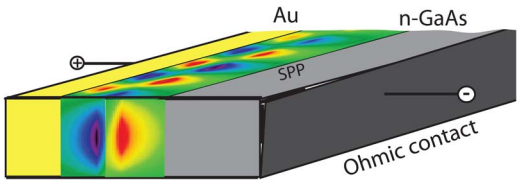

DOI: 10.1109/JPHOT.2013.2256114
1943-0655/$31.00 ©2013 IEEE

IEEE photonics SOCIETY

IEEE

Surface Plasmon Polaritons Propagation Through a Schottky Junction: Influence of The Inversion Layer

T. M. Wijesinghe, *Member, IEEE*, and M. Premaratne, *Senior Member, IEEE*

Advanced Computing and Simulation Laboratory (AχL), Department of Electrical and Computer Systems Engineering, Monash University, Clayton, VIC 3800, Australia

DOI: 10.1109/JPHOT.2013.2256114
1943-0655/$31.00 ©2013 IEEE

Manuscript received February 13, 2013; revised March 22, 2013; accepted March 25, 2013. Date of publication April 4, 2013; date of current version April 17, 2013. The authors would like to thank Australian Research Council for the financial support. Corresponding author: T. M. Wijesinghe (e-mail: wijesinghet@gmail.com).

Abstract: Surface plasmon polaritons (SPPs) originate from resonance coupling between surface-bound electrons and photons on interfaces with specific material properties. Unfortunately, owing to the existence of SPPs on an interface, its reach is plagued by intrinsic dissipative losses in the materials making up the interface, severely restricting the application domain. One way to reduce the propagation losses is to use distributed electrical injection across the interface to create a population inversion to provide energy to the decaying SPP wave. A promising technique is to use a Schottky junction formed between a semiconductor and a metal because such an interface can sustain a population inversion under electrical injection. We previously analyzed the plasmonic dispersion relation for such a device when biased. Here, we extend that analysis to consider the influence of the inversion layer when minority carriers are injected from an external electrical source. In particular, we derive analytical expressions for the loss reduction and associated gain spectrum broadening, taking into account the doping concentration in the semiconductor and the externally applied voltage across the junction. Our analysis gives vital information for the design and utilization of Schottky junction interfaces as active waveguides for routing SPPs in integrated circuitry.

Index Terms: Active plasmonics, material gain, modal gain, Schottky junction.

1. Introduction

Collective electron oscillations in metal-like materials are known as plasmons. A coupled state between a plasmon and a photon on a material interface is commonly referred to as a surface plasmon polariton (SPP) [1]–[3]. Owing to having the wavelength in the μm range, the infrared light cannot be effectively utilized in nanoscale. SPPs have been proven to be effective in nanoscale because they are malleable to the extent to navigate through nanoscale "holes" and "trenches," overcoming constraints imposed by the fundamental diffraction limit [4]. Thus, SPPs have found applications in wide range of areas such as circuitry [5], [6], microscopy [7], spectroscopy [8], imaging [9], biosensing [10], nanolithography [11], solar cells [12], and metamaterials [13], [14]. However, the field enhancements and propagation distances associated with SPPs are limited due to intrinsic losses in the material making up the interface. Therefore, these losses seen by the surface wave must be reduced by transferring energy from an external source to the interface wave [1], [15]. The simplest way to achieve this energy transfer is to utilize the stimulated emission process to clone a fraction of the propagating interface-bound photons by using a suitable gain

medium adjacent to the interface [15]. Such gain-assisted SPP propagation has been studied in many contexts in literature, e.g., planar metal stripe waveguides [16], nanoparticles [17], [18], nanospheres, nanowires [19], gratings [20] incorporating gain media contain dye molecules [21], polymers [22], quantum dots [23], and semiconductors [24]–[26].

The simplest surface that can sustain an SPP has very clearly identifiable materials making up the interface. Usually dielectrics are paired with metals to form the interface, sustaining a permittivity discontinuity at the interface. Rightfully in such a case, it is assumed (and experimentally observed) that no measurable change in the materials occurs due to the formation of the interface. Therefore, freestanding material permittivity values are used in the analysis of the properties pertaining to the creation of the interface. However, owing to carrier exchange between the contacting materials, this assumption breaks down if an interface is made between a metal and a semiconductor, which is commonly known as a Schottky junction. Under certain conditions, such an interface can sustain an SPP mode [27]. Perhaps more intriguingly, a Schottky junction can sustain a population inversion under electrical injection and possesses the ability to strengthen the decaying surface wave using the stimulated emission process. This mechanism is successfully exploited in several recent publications [24], [27]–[29] to extend the propagation lengths of SPPs.

Since the discovery of "unilateral conduction" of crystals by German scientist Karl Ferdinand Braun, the metal–semiconductor junctions are widely used in electrical power industry and signal processing. Greater understanding of its operation was achieved after a publication by Schottky in 1938 [30], [31], which eventually enabled to engineer the device for mass-scale production. Thus, it is widely known as the Schottky (junction) diode. In plasmonics, the replacement of the conventional passive dielectric making up the SPP-bound interface by an active semiconductor demands much thought and care. Especially, this is due to the fact that there is a measurable difference/distinction between the physical discontinuity of the materials and the electrical and optical properties. Owing to the exchange of charge through the interface to establish thermodynamic equilibrium conditions, in the vicinity of the physical interface, there exists a space-charge region in the semiconductor side. However, the availability of essentially a large pool of electrons in the metal washes out the appearance of a space-charge region in the metal side. Interestingly, owing to the presence of this space-charge region in the semiconductor side, some of the interface properties can be changed by an externally applied potential difference across the junction, making it very attractive for modern plasmonic applications. This space-charge region also possesses a substructure, which can be described as a combination of a depletion layer and an inversion or an accumulation layer, where each layer contributed differently to SPP propagation [27]. A considerable body of theoretical and experimental work on SPP behavior in these charge layers has been carried out during the last few decades [32]–[36]. Notably, the role of inversion layer for providing gain in semiconductor medium is emphasized in the work of Fedyanin *et al.* [24], [28], which we further analyzed by devising a technique to calculate the SPP dispersion relation under bias conditions [27].

In this paper, we analyze the space-charge regions induced by the metal–semiconductor interface and its deformation by an externally applied bias voltage yielding the stimulated emission process. Our main focus is to extend the SPP field propagation length by reducing losses. Bearing that goal in mind, we consider minority carrier injection into the Schottky junction and formation of an inversion layer in the semiconductor boundary. In studying the properties of surface space-charge layers consisting of either accumulation or inversion layers, whenever possible, we have deviated from the straightforward numerical analysis to provide approximate analytical solutions, giving much insight and understanding [24], [28], [37]–[39]. Especially, we analyze the mathematical relations given for carrier concentrations in the space-charge region under degenerate conditions by solving the Poisson equations. Then we quantitatively analyze the stimulation emission rate in the inversion region experienced by SPP field propagate in the metal–semiconductor interface.

2. Formation of the Inversion Layer

It is not only instructive, but to set the scene for the following analysis, we also first discuss the formation of the inversion layer in a Schottky junction under forward voltage bias. To simplify the

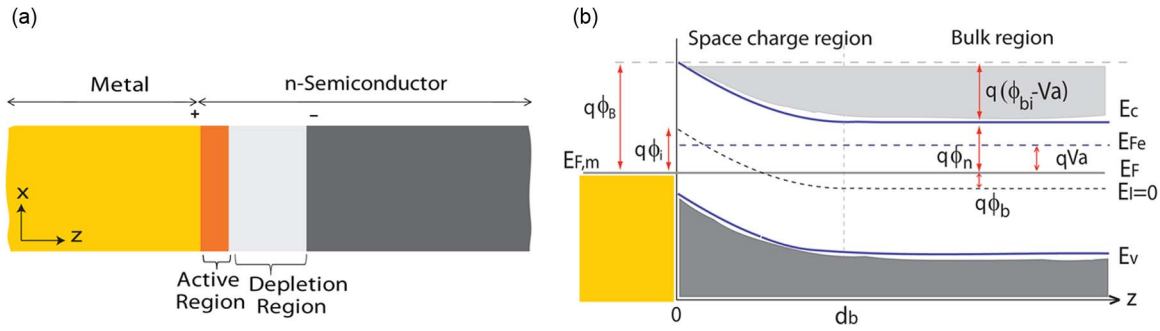

Fig. 1. (a) The metal–semiconductor (Schottky) junction with an active region. (b) The energy band diagram of the Schottky junction. The variable are defined in the Section 2.

analysis and use the machinery of semiclassical analysis to present the main ideas clearly without clutter, we discard the spontaneous emission within the junction. Essentially, in any complex setup on which optical gain occurs as a result of stimulated emission, it is possible to identify two (nondegenerate) energy levels of the active atoms of the gain medium: an upper and a lower energy level. When these levels are bathed in an electromagnetic field with energy matching the difference between the upper and lower levels, stimulated emission can take place by cloning incoming photons. According to Einstein's formulation of the stimulated emission (i.e., Einstein's B coefficient), the stimulated emission rate is proportional to the number of excited atoms in the upper level [1]. Therefore, for the stimulated emission to dominate, having an excess of excited atoms in the upper level compared to the lower level is required, which is commonly referred to as "population inversion" condition. The region where such a population inversion happens is named as an inversion layer.

Whenever a contact is made between a metal and a semiconductor, mobile carriers flow from one to the other until their Fermi levels are aligned as demanded by thermodynamic conditions. These charge movements disturb the charge neutrality conditions and create a space-charge region in the vicinity of the interface, generating an electric field across the interface (or junction) [40]. Conversely, we could also apply an external electric field across the junction and manipulate the space-charge region shape, extent, and properties [40]. The properties of space-charge layers associated with semiconductor junctions are normally calculated in an approximate manner by using the depletion approximation [41], whereby the space-charge region is assumed to be completely depleted of mobile electrons and holes. But this is not always true as depending on the surface potential, doping concentration, and biased voltage, there could be a carrier surplus forming an inversion or an accumulation layer near the metallurgical junction [37], [42]–[44]. In the micro- and nanoscale, these carrier distribution changes cannot be neglected. Here, we pay our attention to inversion regions, which leads to the carrier recombination process. An inversion layer is always accompanied by a depletion region [42], [45], [46]. In a depletion region, the bound impurity charge dominates, while in an inversion or accumulation layer, the free charge dominates.

In this paper, without loss of generality, we consider a Schottky junction formed by a metal and an n-type semiconductor as shown in Fig. 1(a) with free hole concentration, p, electron concentration, n, and donor doping concentrations, N_D. Suppose the Schottky junction is forward biased so that the condition for a p-type inversion layer, $p - n \gg N_D$, is satisfied. In this paper, the carrier densities in the space-charge region are analyzed assuming semiconductor under degenerate conditions. Degeneracy is obtained by heavily doping the semiconductor so then its Fermi level stays closer to the band edge (conduction or valence) by less than a magnitude of $2KT/q$. Here, K, T, and q are the Boltzmann's constant, absolute temperature, and electron charge. The properties of degenerate semiconductors must be described using the Fermi–Dirac statistics instead of the Maxwell–Boltzmann statistics [41]. Since the minority carrier density in the inversion region could rise above the donor concentration and effective density of states, the simplified Boltzmann approximation is invalid in this scenario. Fig. 1(b) shows the energy band diagram for the Schottky junction

considered in this paper. We assign coordinates x along the interface and z across the interface with origins as marked [see Fig. 1(a)]. Here, E_c and E_v are the conduction and valence energy bands. E_F defines the Fermi energy level while E_{Fe} is the quasi-Fermi level of electrons. E_I is the intrinsic energy level, which is considered as the zero reference level. Then, at any point of the semiconductor, the potential is defined as

$$\phi = \frac{(E_F - E_I)}{q}$$

which is then normalized to

$$u = \frac{q\phi}{KT}. \tag{1}$$

Also, the electric field, $F = -d\phi/dz$, can be normalized as

$$\xi = \frac{qF}{KT}.$$

The notation for the energy difference between points P and Q is given by

$$w_{P,Q} = \frac{(E_P - E_Q)}{q}.$$

Then at any point in the semiconductor crystal, the concentration of electrons in the conduction band is defined by

$$n = 2\int_{E_c}^{\infty} D_c(E) f(E)\, dE \tag{2}$$

where $D_c(E)$ is the density of states of conduction band given by, [41], [47]

$$D_c(E) = 2\pi\left(\frac{2m_n^*}{h^2}\right)^{3/2}(E - E_c)^{1/2}.$$

Here, m_n^* and h are the effective mass of electrons in the conduction band and Plank's constant. $f(E)$ is the Fermi–Dirac distribution defined by

$$f(E) = \frac{1}{1 + e^{(E-E_F)/KT}}. \tag{3}$$

Then (2) can be written in the form

$$n = 4\pi\left(\frac{2m_n^*}{h^2}\right)^{3/2}\int_{E_c}^{\infty}\frac{(E - E_c)^{1/2}}{1 + e^{(E-E_F)/KT}}\, dE.$$

By rearranging variables

$$n = \frac{2}{\sqrt{\pi}} N_c F_{\frac{1}{2}}\left(\frac{E_F - E_c}{KT}\right). \tag{4}$$

This can be written in terms of normalized potentials as

$$n = \frac{2}{\sqrt{\pi}} N_c F_{\frac{1}{2}}(u - w_{C,I}) \tag{5}$$

where $F_j(\eta)$ is the Fermi–Dirac integral defined by [41], [47], [48]

$$F_j(\tau) = \int_0^\infty \frac{\chi^j d\chi}{1 + e^{\chi - \tau}}.$$

Here, χ and τ are real values and j defined the order of the integral. In an analogous manner, at any point, the concentration of holes in the valence band is given by

$$p = \frac{2}{\sqrt{\pi}} N_v F_{\frac{1}{2}}(w_{V,I} - u) \tag{6}$$

where $N_c = 2(2m_n^* KT/h^2)^{3/2}$ and $N_v = 2(2m_p^* KT/h^2)^{3/2}$ are the effective densities of states of conduction and valence bands. The concentration of electrons due to ionized impurities can be derived as [41]

$$n_D = \frac{N_D}{1 + 2e^{(E_D - E_F)/KT}}$$

where E_D is the electron energy level of donors. Then charge density can be written in the normalized form in the following:

$$\rho_D = \frac{qN_D}{1 + 2e^{(u - w_{D,I})}}.$$

For this charge distribution, the Poisson's equation can be written in terms of u using (1)

$$\frac{d^2u}{dz^2} = -\frac{q}{KT}\frac{\rho}{\epsilon}. \tag{7}$$

For an n-type semiconductor, considering minority and majority carriers and donor impurities

$$\rho = \rho_D + q(p - n).$$

A second-order differential equation can be obtained for the normalized potential by substituting ρ into (7) in the following form:

$$\frac{d^2u}{dz^2} = -\frac{1}{2L_D^2}\left[\frac{N_D}{n_i(1 + 2e^{(u - w_{D,I})})} + \frac{F_{\frac{1}{2}}(w_{V,I} - u)}{F_{\frac{1}{2}}(w_{V,I})} - \frac{F_{\frac{1}{2}}(u - w_{C,I})}{F_{\frac{1}{2}}(w_{I,C})}\right] \tag{8}$$

where $L_D = \sqrt{\epsilon^s kT/2q^2 n_i}$, ε^s, and n_i are the intrinsic Debye length, permittivity of the semiconductor, and intrinsic carrier density defined by

$$n_i = \frac{2}{\sqrt{\pi}} N_c F_{\frac{1}{2}}(w_{V,I}) = \frac{2}{\sqrt{\pi}} N_v F_{\frac{1}{2}}(w_{I,C}).$$

Equation (8) can be solved numerically as a boundary value problem for known E_c, E_v, E_D, N_D, and n_i values [49]. Considering boundary conditions according to Fig. 1(b), the potential at the bulk semiconductor faraway from the interface is given by

$$q\phi_b = E_{F_{\text{bulk}}} - E_I = E_c - \phi_n.$$

Here, $\phi_n = (E_c - E_F)/q$. Then the normalized potential at the bulk including a forward biased applied voltage V_a can be written in the form

$$u_b = \frac{E_c - \phi_n}{KT} + \frac{qV_a}{KT}.$$

Since $n = N_D$ at the bulk, using (4)

$$E_c - E_F = q\phi_n = -\frac{KT}{q}\left[\ln\left(\frac{N_D}{N_c}\right) - 2^{-3/2}\ln\left(\frac{N_D}{N_c}\right)\right].$$

To find the space-charge width d_b, let us consider the full depletion approximation and apply Poisson's equation

$$\frac{d^2u}{dz^2} = -\frac{q}{KT}\frac{\rho}{\epsilon}, \quad \frac{d^2u}{dz^2} = -\frac{q^2N_D}{KT\epsilon} = -\frac{1}{L_e}$$

where $L_e = \sqrt{KT\epsilon/q^2N_D}$ is the extrinsic Debye length. Now integrating from z to d_b

$$\int_z^{d_b}\frac{d^2u}{dz^2}dz = -\frac{1}{L_e^2}\int_z^{d_b}dz, \quad \frac{du}{dz} = \frac{1}{L_e^2}(d_b - z).$$

By integrating again and substituting $z = 0$

$$d_b^2 = L_e^2(u_b - u_i).$$

Now let us consider the potential at the interface according to Fig. 1(b)

$$q\phi_i = E_{F_{\text{int}}} - E_I = -(q\phi_B - E_c).$$

Then the normalized potential at the interface including a forward biased applied voltage is given by

$$u_i = -\frac{q\phi_B - E_c}{KT} - \frac{qV_a}{KT}$$

where ϕ_B is the Schottky barrier height. The built-in potential of a degenerate n-type semiconductor–metal junction can be stated as

$$q\phi_{bi} = q\phi_B - q\phi_n.$$

Similarly, the normalized built-in potential including an applied voltage can be written as

$$u_{bi} = \frac{q\phi_B - q\phi_n}{KT} - \frac{qV_a}{KT}.$$

To find the normalized electric field $\xi = -du/dz$, let us consider (8). Now integrating from z to d_b

$$-L_D^2\left(\frac{du}{dz}\right)^2 = \frac{N_D}{n_i}\ln\left[1 + \frac{1}{2}e^{(w_{D,I}-u)}\right]_u^{u_b} - \frac{2}{3}\left[\frac{F_{\frac{3}{2}}(w_{V,I} - u)}{F_{\frac{1}{2}}(w_{V,I})}\right]_u^{u_b} + \frac{2}{3}\left[\frac{F_{\frac{3}{2}}(u - w_{C,I})}{F_{\frac{1}{2}}(w_{I,C})}\right]_u^{u_b} = I. \tag{9}$$

The integration is performed using the fact that for $j > 0$, $\partial F_j(\tau)/\partial\tau = jF_{j-1}(\tau)$. Then the electric field at interface can be found from (9) using $\xi_i = -(du/dz)_{u=u_i}$ given that $(du/dz)_{u=ub} = 0$ at the bulk. An expression for normalized potential in terms of position can be obtained by rearranging variables and integrating (9) from the interface toward the bulk

$$\frac{z}{\sqrt{2}L_D} = \int_{u_i}^{u}\frac{du}{\sqrt{I}}. \tag{10}$$

Equation (10) is solved numerically and the potential variation across the space-charge region in the Schottky junction is found [49]. Then using (5) and (6), the carrier profiles are obtained. Fig. 2 illustrates the potential and the minority carrier distribution in the space-charge region and its dependence with the applied voltage V_a and donor concentration N_D. The numerical data are

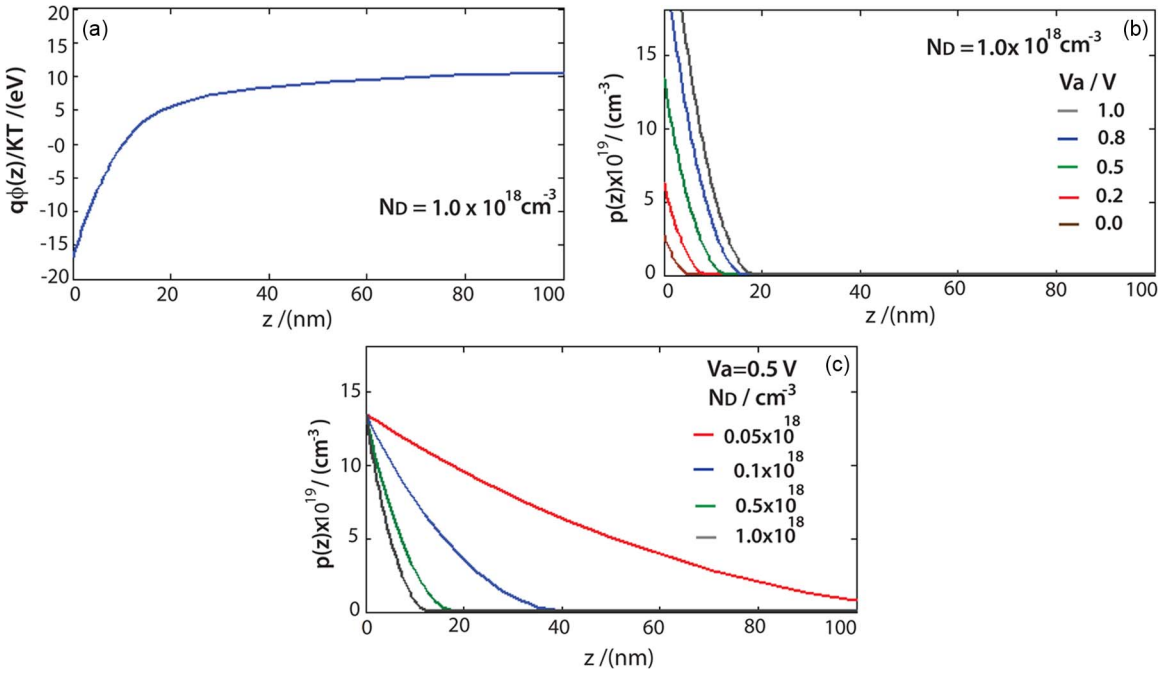

Fig. 2. (a) The normalized potential variation in the space-charge region. (b) The minority carrier density variation in the space-charge region for different applied voltages with a donor density of 1×10^{18} cm^{-3} and (c) for different donor densities with an applied voltage of $V_a = 0.5$ V.

considered for Au–GaAs junction assuming $\phi_B = 0.85$ eV, $\varepsilon^s = 11.9$, $KT = 4.14 \times 10^{-21}$ J, $E_c - E_v = 1.42$ eV, $E_D = 0.01$ eV, $n_i = 1 \times 10^6$ cm^{-3}, $N_c = 4 \times 10^{17}$ cm^{-3}, and $N_v = 1 \times 10^{18}$ cm^{-3}. As shown in Fig. 2(a), at the junction, the potential is negative but increases positively toward the bulk region. The width of the inversion region is increasing with the applied voltage [see Fig. 2(b)] and decreasing with the doping concentration as depicted in Fig. 2(c). Yet the total width of the space-charge region reduces with applied voltage since the potential barrier reduces as the junction is forward biased. The results obtained in Fig. 2 are quantitatively agreed with the numerical results in [38], [50].

3. Stimulated Emission Resulting From the Inversion Layer

A passive semiconductor material can be made an active one by pumping energy optically or electrically by means of creating a nonequilibrium carrier distribution. This population inversion condition can supply energy gain to the nearby photons with energies exceeding the material's bandgap energy. This scenario can simply elaborate by considering the semiconductor material as a two-level system with upper levels in the conduction band and lower levels in the valence band. The photon energy $\hbar\omega$ of incident light field defines the electron transition between these two levels. Here, $\hbar = h/2\pi$ and ω is the optical carrier frequency. The rates of absorption and emission between lower and upper states are governed by the relative carrier densities in the sample. When the density of carriers in some lower energy state E_a exceeds the density of carriers in some upper state $E_b = E_a + \hbar\omega$, there is a photon of energy $\hbar\omega$ that will stimulate a transition from the lower state to the upper state. Also, a photon can stimulate a transition from the upper state to the lower state. Usually, the absorption is more probable than stimulated emission. It means that the intensity of an optical field decreases as it passes through the material because of the net absorption. But under the population inversion condition, stimulated emission is more probable than stimulated absorption and the intensity of the optical field increases as it passes through the material. This is called the gain.

By electrical or optical carrier injection, carrier densities of the upper and lower states can be varied resulting gain or absorption [51]. The carrier transitions are decided by wave-vector selection

and polarization selection rules. Here, we study the electromagnetic field interaction with the gain media in order to find solutions to compensate or amplify desired signals. When a semiconductor is illuminated by an electromagnetic field, the interaction between photons and electrons in the semiconductor is described by the Hamiltonian [48]. Accordingly, from the time-dependent perturbation theory [47] and the Fermi golden rule [48], the absorption coefficient is defined by

$$\alpha(\omega) = C_o \Sigma_k |\hat{e}.P_{cv}|^2 \delta[E_c(k) - E_v(k) - \hbar\omega]\{f_v[E(k)] - f_c[E(k)]\}$$

given

$$C_o = \frac{\pi q^2}{n^s c \epsilon_o m_o^2 \omega}.$$

The symbols ε_o, c, m_o, k, $\hat{e}$, and P_{cv} are the permittivity of vacuum, speed of light in vacuum, electron mass, wave vector, unit vector along the propagation direction, and the momentum matrix [47] between conduction and valence bands. Also, $f_v[E(k)]$ and $f_c[E(k)]$ are the Fermi–Dirac distributions of valence and conduction bands defined by equation (3) where E_F becomes E_{Fh} and E_{Fe}, respectively, which are the quasi-Fermi levels of holes and electrons. Moreover, the value of $\alpha(\omega)$ can be made negative if $f_v[E(k)] - f_c[E(k)] < 0$, which leads to

$$e^{(E_v - E_{Fh})/KT} - e^{(E_c - E_{Fe})/KT} < 0, \qquad E_{Fe} - E_{Fh} > \hbar\omega \geq E_c - E_v.$$

For the population inversion, this condition must be satisfied and then absorption coefficient becomes negative, which results in a gain in the medium. The gain $g(\omega)$ can be existed for SPP frequencies for which the photon energy $\hbar\omega$ is smaller than the Fermi level splitting. Then

$$g(\omega) = -\alpha(\omega).$$

Now considering the parabolic approximation for energy dispersions of conduction and valence bands

$$E_c(k) = E_c + \frac{\hbar^2 k^2}{2m_e}, \quad E_v(k) = E_v - \frac{\hbar^2 k^2}{2m_h}$$

where

$$\frac{1}{m_r} = \frac{1}{m_e} + \frac{1}{m_h}.$$

As defined in Section 2, E_c and E_v mean the minimum energy of conduction band and the maximum energy of valence band, respectively. Here, m_e, m_h, and m_r are the mass of an electron, the mass of a hole, and the reduced effective mass. Then $\alpha(\omega)$ can be evaluated in the form

$$\alpha(\omega) = C_o |\hat{e}.P_{cv}|^2 \frac{1}{2\pi^2} \left(\frac{2m_r}{\hbar^2}\right)^{3/2} \sqrt{\hbar\omega - E_g}\{f_v[E(k)] - f_c[E(k)]\}, \tag{11}$$

where $E_g = E_c - E_v$ and $k = 2m_r/\hbar^2(\hbar\omega - E_g)$. Moreover, considering the interaction of the electron–hole pair, the absorption coefficient under externally applied uniform electric field ξ (given $\xi = qF/KT$) is defined as [48]

$$\alpha(\omega) = \frac{B_o}{2\pi} \left(\frac{2m_r^*}{\hbar^2}\right)^{3/2} \sqrt{\hbar\theta_\xi}\left[-\eta \mathrm{Ai}^2(\eta) + \mathrm{Ai}'^2(\eta)\right],$$

where

$$B_o = C_o |\hat{e}.P_{cv}|^2 = \frac{\pi q^2 |\hat{e}.P_{cv}|^2}{n_s c \epsilon_o m_o^2 \omega}.$$

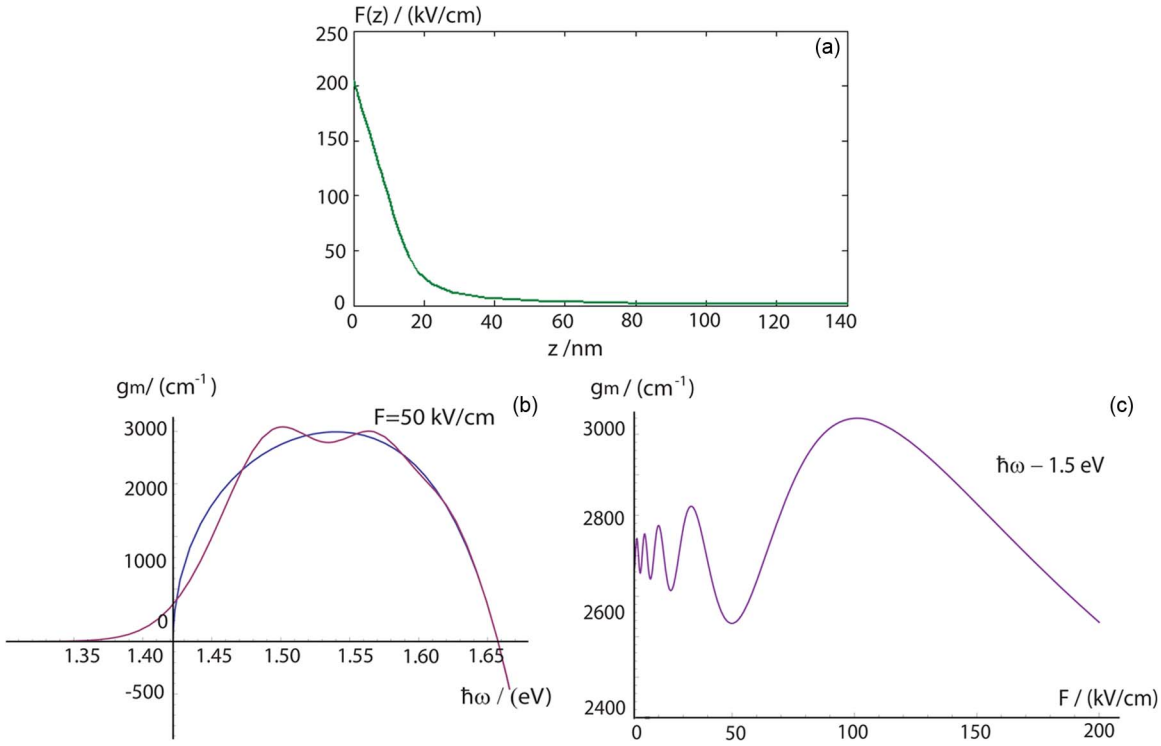

Fig. 3. (a) The variation of static electric field along the junction ($V_a = 0.8$ V). (b) The gain spectrum for $F = 0$ and $F = 50$ kV/cm. (c) The gain variation with externally applied electric field for $\hbar\omega = 1.5$ eV. Also, $N_D = 1.0 \times 10^{18}$ cm^{-3} and $p = 0.5 \times 10^{20}$ cm^{-3}. Other parameters are selected for GaAs.

Here, $\hbar\theta_\xi = (\hbar^2 K^2 T^2 \xi^2 / 2m_r^*)^{1/3}$ and $\eta = (E_g - \hbar\omega)/\hbar\theta_\xi$. The symbol $\mathrm{Ai}(\eta)$ defines the Airy function with respect to η. The absorption spectrum under externally applied electric field expands the spectrum below the band edge (broadening the absorption/gain spectra) and showing oscillatory behavior. This is known as the Franz–Keldysh effect [47], [48]. As depicted in Fig. 3(a), the higher carrier inversion level increases the corresponding static electric field near the contact compared to the depletion region. Under the forward biased condition, this field causes to broaden the gain spectrum of the semiconductor. Fig. 3(b) illustrates the variation of the material gain spectrum of an n-type Schottky junction with and without the presence of an external electric field. As it clearly shows, when subjected to an external field, $F = 50$ kV/cm, the gain spectrum extends below the bandgap energy of GaAs (i.e., below 1.42 eV). However, above E_g, a slight oscillation of the spectrum can be noticed. In Fig. 3(c), we plot this oscillatory behavior when the applied electric field is in the range 0–200 kV/cm.

In (11), the Fermi–Dirac distributions are obtained using Fermi levels of electrons and holes in the semiconductor. The Fermi levels define the free electron concentration and hole concentration. The inverse formulas of (5) and (6) are used to find the Fermi levels [41]. For known hole concentration, E_{Fh} can be found by

$$E_v - E_{Fh} \approx KT\left[\ln\left(\frac{p}{N_v}\right) + 2^{-3/2}\ln\left(\frac{p}{N_v}\right)\right].$$

For an n-type Schottky junction with a p-type inversion region, $n(z)$ is calculated using the donor concentration and $p(z)$ is calculated from (6). The optical gain spectrum for n-type Schottky junction is shown in Fig. 4(a) for different N_D and p values ($E_g = 1.42$ eV for GaAs at $T = 300$ K). For selected $\hbar\omega$ and N_D values, the semiconductor material gain can be approximated by a linear function when the carrier densities are quite close to N_v

$$g_m(z) = g_t(p(z) - p_t).$$

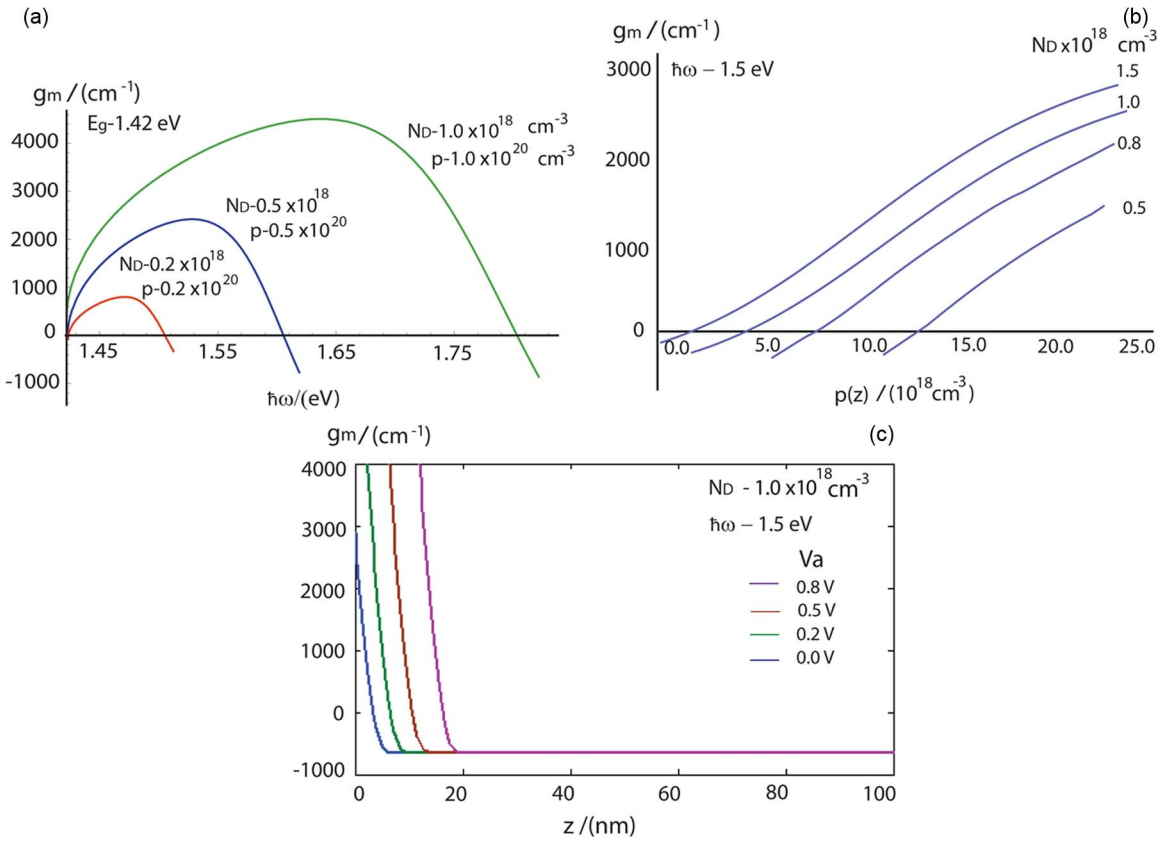

Fig. 4. (a) Material gain spectrum of the Schottky junction for different values of N_D and p. (b) Material gain variation with minority carrier density along z. (c) Material gain variation along z for different forward biased voltages. Also, $\hbar\omega = 1.5$ eV and $N_D = 1.0 \times 10^{18}$ cm^{-3}. Other parameters are selected for GaAs at 300 K.

The symbols g_t and p_t are the differential gain and the transparency density that can be calculated numerically according to Fig. 4(b), which shows the material gain variation against the minority carrier density, $p(z)$, for different donor densities, N_D. When the carrier densities are considerably larger than N_v, the gain variation can be fitted to a logarithmic function improving the accuracy

$$g_m(z) = g_o\left(\ln\left[\frac{p(z)}{p_o}\right] + 1\right). \tag{12}$$

Here, g_o and p_o are constant parameters where $p = p_o e^1 = p_t$ when $g_m(z) = 0$ and $g_m(z) = g_o$ when $p = p_o$. In Fig. 4(c), the variation of material gain with distance z is shown for $\hbar\omega = 1.5$ eV and $N_D = 1.0 \times 10^{18}$ cm^{-3} at different forward biased voltages. As the inversion width increases with the forward bias voltage, it increases the stimulated emission rate. Hence, the interaction of optical field with the active layer increases with the biased voltage. The results in Fig. 4 illustrate quite a similar behavior to the numerical results obtained in [28].

4. Impact of the Inversion Layer on the SPP Mode

SPP propagation has been widely analyzed for heterostructures such as PN junctions and Schottky junctions in order to have efficient integrating techniques of plasmonic systems with electronic circuits. SPP dispersion relations and field profiles are commonly studied for metal and dielectric setup. The same approach is used here for metal–semiconductor interface assuming

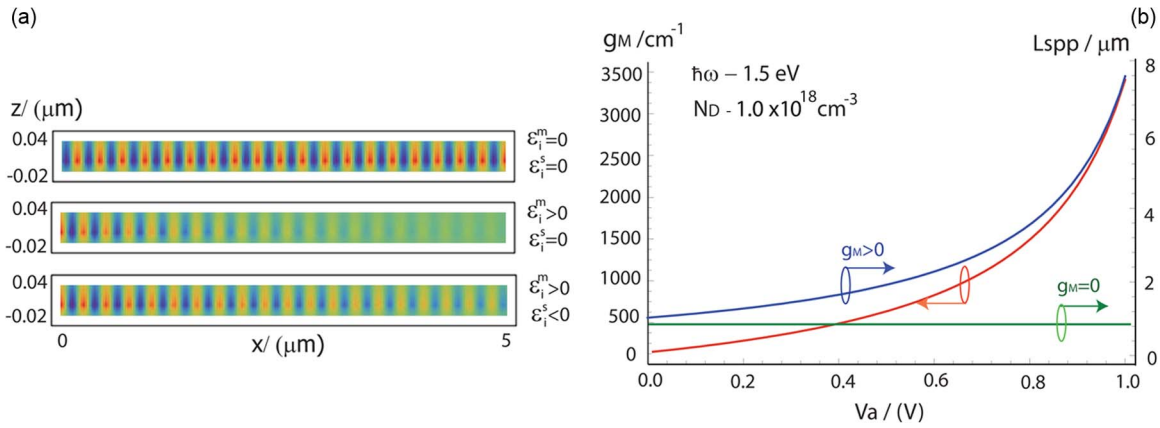

Fig. 5. (a) $H_y(z)$ component of the TM_{00} SPP mode for different values of ε_i^m and ε_i^s. (b) The variation of modal gain with applied junction voltage (left). The variation of L_{spp} with the applied junction voltage with and without the gain effect (right).

semiconductor as an active medium. Considering TM_{00} SPP mode propagates along a metal–semiconductor interface (x-direction), the Maxwell's equations can be reduced into the following form [2], [3]:

$$F_x = -i\frac{1}{\omega\varepsilon_o\varepsilon}\frac{\partial H_y}{\partial z}, \quad F_z = -\frac{\beta}{\omega\varepsilon_o\varepsilon}H_y.$$

Then the wave equation for TM_{00} mode is written by

$$\frac{\partial^2 H_y}{\partial z^2} + \left(k_o^2\varepsilon - \beta^2\right)H_y = 0. \tag{13}$$

F_x, F_z, and H_y are the electric field and magnetic field components of TM_{00} SPP mode. Here, $k_o = \omega/c$ is the optical wave vector in vacuum. For the metal (m) and semiconductor (s), SPP mode solutions can be derived as

$$H^{s,m}(x,z) = (0,b,0)e^{I\left(\beta x + k_z^{s,m} z - \omega t\right)}, \quad F^{s,m}(x,z) = \left(\frac{ibk_z^{s,m}}{\omega\varepsilon_o\varepsilon^{s,m}}, 0, \frac{b\beta}{\omega\varepsilon_o\varepsilon^{s,m}}\right)e^{i\left(\beta x + k_z^{s,m} z - \omega t\right)}.$$

The symbol b is a normalization constant that can be found using the total power flow in the system [2]. The symbols β and $k_z^{s,m}$ are the complex longitudinal and transverse propagation vectors of the SPP mode. Then by applying continuity conditions at the junction, the SPP dispersion relation can be derived as follows:

$$\beta = \frac{\omega}{c}\frac{\left(\varepsilon_r^m + i\varepsilon_i^m\right)\left(\varepsilon_r^s + i\varepsilon_i^s\right)}{\left(\varepsilon_r^m + i\varepsilon_i^m\right) + \left(\varepsilon_r^s + i\varepsilon_i^s\right)}.$$

Here, $\varepsilon_r^m + i\varepsilon_i^m$ and $\varepsilon_r^s + i\varepsilon_i^s$ are the complex metal and semiconductor permittivities, respectively. The imaginary component, ε_i^m, leads to lossy propagation while having a negative ε_i^s can cause an energy gain to the field [see Fig. 5(a)]. Generally the variation in propagation vector due to the change in permittivity is studied using the perturbation approach, which can be derived using the wave equation [27]. By multiplying (13) with complex conjugate of H_y and integrating from minus to plus infinity, the following expression can be obtained [48]:

$$\beta^2 \int_{-\infty}^{\infty} H_y(z)H_y^*(z)dz = k_o^2 \int_{-\infty}^{\infty} \varepsilon(z)H_y(z)H_y^*(z)dz + \int_{-\infty}^{\infty} H_y^*(z)\frac{\partial^2 H_y(z)}{\partial z^2}dz. \tag{14}$$

The right-hand side of the equation can be rewritten as

$$\int_{-\infty}^{\infty} H_y^*(z)\frac{\partial^2 H_y(z)}{\partial z^2}dz = \left[H_y^*(z)\frac{\partial H_y(z)}{\partial z}\right]_{-\infty}^{\infty} - \int_{-\infty}^{\infty}\left|\frac{\partial H_y(z)}{\partial z}\right|^2 dz. \tag{15}$$

For guided modes, assume both $H_y^*(z)$ and $\partial H_y(z)/\partial z$ vanish as $|z| \to \infty$. Then the first term on the right-hand side of (15) can be made zero. The second term is positive definite [52]. Thus the imaginary part of (14) can be written as

$$(\beta^2)_i = \frac{k_o^2 \int_{-\infty}^{\infty} \Delta\varepsilon_i(z) H_y(z) H_y^*(z) dz}{\int_{-\infty}^{\infty} H_y(z) H_y^*(z) dz}.$$

β can be written in terms of its real (β_r) and imaginary $(\Delta\beta_i)$ components

$$\beta^2 = (\beta_r + i\Delta\beta_i)^2 = \beta_r^2 - \Delta\beta_i^2 + 2i\beta_r\Delta\beta_i$$

then

$$(\beta^2)_i = 2\beta_r\Delta\beta_i.$$

Hence, the perturbation of complex propagation vector due to permittivity change can be written as

$$\Delta\beta_i = \frac{k_o^2 \int_{-\infty}^{\infty} \Delta\varepsilon_i(z) H_y(z) H_y^*(z) dz}{2\beta_r \int_{-\infty}^{\infty} H_y(z) H_y^*(z) dz}. \tag{16}$$

The joule loss coefficient for SPP is defined as $\alpha_j = 2\Delta\beta_i$ [15]. Then

$$\alpha_j = \frac{k_o^2 \int_{-\infty}^{0} \Delta\varepsilon_i(z)\left|H_y(z)\right|^2 dz}{\beta_r \int_{-\infty}^{\infty}\left|H_y(z)\right|^2 dz}.$$

The integral in the numerator is carried out over the area of metal considering only the ohmic losses. Now consider SPP mode propagation in an active medium. The complex permittivity can be given in terms of material gain g_m as $\varepsilon_i^s(z) = n_s c g_m(z)/\omega$ [15]. The actual gain experienced by the guided SPP mode is known as the modal gain g_M, which can also be written in terms of complex propagation vector as $g_M = 2\Delta\beta_i$ [53]. Then from (16)

$$g_M = \frac{k_o n_s \int_0^{d_b} g_m(z)\left|H_y(z)\right|^2 dz}{\beta_r \int_{-\infty}^{\infty}\left|H_y(z)\right|^2 dz}. \tag{17}$$

Here, the integral in the numerator is carried out only over the area of the space-charge region and the integral in the denominator is carried out over the entire cross section of the mode. Thus, the net absorption is given by the difference of α_j and g_M. As given $\beta = k_o n_{eff}$, the modal loss and gain can be written in terms of effective index, n_{eff}, and the material gain. The net absorption can be written in the form

$$\alpha_{net} = \frac{k_o \int_{-\infty}^{0} \Delta\varepsilon_i(z)\left|H_y(z)\right|^2 dz}{n_{eff} \int_{-\infty}^{\infty}\left|H_y(z)\right|^2 dz} - \frac{n_s \int_0^{d_b} g_m(z)\left|H_y(z)\right|^2 dz}{n_{eff} \int_{-\infty}^{\infty}\left|H_y(z)\right|^2 dz}.$$

The variation of modal gain with applied voltage is shown in Fig. 5(b)-(left). The space-charge region in the Schottky junction is formed by the electron depletion from the semiconductor to the metal. When the junction becomes forward biased, an inversion layer is formed, which creates a great supply of minority carriers (holes) near the contact exceeding the concentration of electrons.

For n-type semiconductor, this happens by bending the valence band beyond the quasi-Fermi level. As the forward biased voltage increases, the inversion region becomes wider as the minority carriers inject to the semiconductor bulk, causing the emission rate to rise up, which makes g_M to be greatly improved giving a chance to partially compensate the SPP power loss. For values $\hbar\omega = 1.5$ eV, $N_D = 1.0 \times 10^{18}$ cm^{-3}, $\varepsilon^m = -35.37 + 2.469i$, and $V_a = 0.8$ V, the rates α_j and g_M are calculated as 4125 cm^{-1} and 1615 cm^{-1} leading $\alpha_{net} = 2510$ cm^{-1}. SPP propagation length is given by $L_{spp} = 1/\alpha_{net}$. The variation of L_{spp} with the applied voltage V_a is shown in Fig. 5(b)-(right), with and without the modal gain in the junction. It can be clearly seen that the semiconductor modal gain provided by inversion region has a vital effect on improving L_{spp} compensating power loss.

5. Discussion

In this paper, we reviewed the relevance and impact of an inversion region formed in a Schottky junction on SPP propagation. As shown in Fig. 2(a), the electrical potential is negative near the contact and gradually increases toward the neutral region. This negative potential is caused by the Fermi level pinning at the contact due to the Schottky barrier. A large concentration of minority carriers can be noted near the contact as shown in Fig. 2(b) for forward biased voltages. This is because at higher forward biased values, drift component of the minority carriers cannot be neglected because it injects a considerable amount of minority carriers to the Schottky junction. This causes a carrier inversion (i.e., p-type region) near the contact. Interestingly, the inversion layer width is bigger for the lightly doped semiconductor. Contrary to this, for the stimulated emission to take place, degenerate conditions are needed. Hence, doping concentration N_D is selected closer to N_c to have a sufficiently strong inversion region to sustain stimulated emission. As shown in Fig. 4(a) and (b), the material gain spectrum of n-GaAs is wider for higher doping densities. Also, according to Fig 2(b), the minority carrier density is considerably higher than N_v for bias voltages over 0.5 V. Hence, the carrier behavior was analyzed for degenerate conditions [see (5) and (6)] and the material gain was calculated using a logarithmic model [see (12)]. The material gain distribution in the junction is shown in Fig. 4(c). As shown in Fig. 2(a) and (b), the width of the space-charge layer could be extended to several hundreds of nanometers while the width of the inversion layer could be extended to few tens of nanometers, depending on the bias voltage. Since this active region is attached to the interface, SPP field is easily captured in the region. The gain experienced by the SPP mode is calculated using (17). As illustrated in Fig. 5(b), for V_a of 0.9 V, g_M can reach around 2500 cm^{-1} improving L_{spp} by a factor of six compared to the passive system.

Our analysis confirms a promising path to use Schottky junction as an active channel for SPP mode propagation. The sample we considered in this paper can be engineered as a single heterostructure Schottky-barrier-diode-based SPP waveguide. The minority carrier surplus near the contact mainly depends on three factors: the Schottky barrier height, the donor density of the semiconductor material, and the biased voltage. As a direct bandgap semiconductor, GaAs is the best candidate for this application to get a high Schottky barrier height when paired with the metal, Au. Au/GaAs contact gives a barrier height of 0.85 eV compared with Ag, Al, and Cu with values of 0.82 eV, 0.75 eV, and 0.78 eV, respectively. Similarly, we have chosen $N_D = 1 \times 10^{18}$ cm^{-1}, a value closer to N_c of GaAs, to achieve degenerate conditions. The operating wavelength was selected as $\lambda = 0.88$ μm $(\hbar\omega = 1.5$ eV$)$ to fall within the range of SPP dispersion frequencies in a Schottky junction. For $N_D = 1.0 \times 10^{18}$ cm^{-3}, $\hbar\omega = 1.5$ eV, and $V_a = 0.8$ V, the waveguide dimensions can be selected with a cross-sectional area of $A = 1.95 \times 0.8$ μm^2 and thickness of $t = 0.8$ μm. Fig. 6(a) shows the schematic diagram of the proposed design. These dimensions were selected considering the maximum skin depth of SPP in each medium to support better confinement. Width of the space-charge region of the semiconductor to support carrier injection and width of the ohmic contact were also considered. Here, the chosen dimensions must be closer to SPP wavelength for efficient nanophotonic applications. These choices give the best performance in terms of practical point of view. However, we can further reduce the waveguide width and thickness values much less than 0.88 μm by concentrating solely on TM_{00} plasmonic mode. Since TM_{00} SPP mode is well confined to the junction compared with TM_{01} and TM_{10} polarizations [55], the inversion layer provides a special

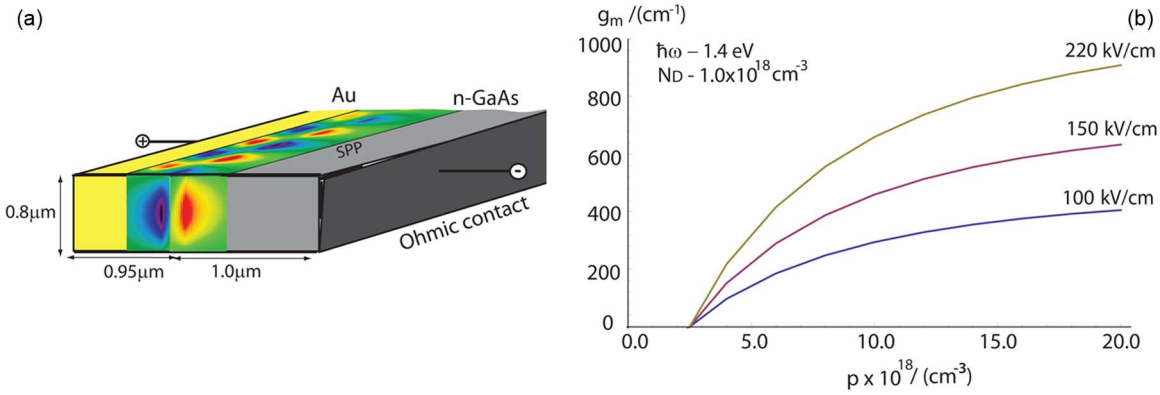

Fig. 6. (a) Schematic diagram of the single heterostructure Schottky-barrier-diode-based SPP waveguide. (b) The variation of material gain with minority carrier density for different values of the applied electric field, F. Here $N_D = 1.0 \times 10^{18}$ cm^{-3} and $\hbar\omega = 1.4$ eV.

localization for the emission, as TM_{00} mode gives the lowest threshold level for the emission process. This device is estimated to operate at moderate current density range of (10–50) kA/cm^2 under forward biased condition. Moreover, the temperature rise in the device due to joule heating can be estimated according to $\Delta T = P_{loss} R_{th}$, where P_{loss} and $R_{th} = t/\sigma A$ are the dissipated power and thermal resistance, respectively [54]. For the sample considered, ΔT is in the range of (0.0001–0.001) K, which has a negligible effect on the emission process. The thermal conductivity of Au, $\sigma = 318$ W/mK at $T = 300$ K.

Moreover, operating in the low-frequency range can considerably reduce the field propagation loss. Hence, consideration of range of emission channels could help improving the device performance. Franz–Keldysh effect extends the gain spectrum to lower energies under an applied static electric field [see Fig. 3(a) and (b)]. For the below bandgap energies, the variation of material gain with minority carrier density is illustrated in Fig. 6(b) for different applied electric fields. The maximum gain increases when the external electric field increases. The average breakdown field for semiconductor junctions is in the range of (300–450) kV/cm; hence, considerable gain can be obtained under normal operating conditions of the junction. Also, by applying a gradually increasing or a nonuniformly varying biased voltage, a uniform SPP field can be obtained via the waveguide by which the device performance can be further improved.

6. Conclusion

As the fundamental element making up SPP circuits, SPP waveguides have been widely investigated in literature. However, only a handful of work have been reported on simple plasmonic structures with active media. In this paper, the influence of inversion layer in the Schottky diode is elaborated and discussed for the gain-assisted SPP waveguiding applications. By injecting minority carriers to the junction using a high forward bias voltage, the formation of an inversion layer near the contact is analyzed in detail. The analytical expressions are derived and solved to study the potential function, carrier densities, and minority carrier profile in the inversion region. The obtained results clearly illustrate the inversion layer close to the junction and its dependence on applied biased voltage and donor density of the semiconductor material. The presence of an inversion layer sustains stimulated emission in the junction, maintaining a gain distribution near the contact. Accordingly the material gain spectrum and approximated gain model for the Schottky diode are discussed. Moreover, a quantitative way to broaden the gain spectrum below the bandgap energy using the static electric field in the junction is discussed. This property can be used to have a range of emission channels in the waveguide to improve the performance. Also, explicit expressions for the modal loss and modal gain of the fundamental SPP mode are defined in order to analyze the net modal gain and SPP propagation length with much ease and control. The results illustrate the improvement of mode propagation length by a factor of six for the considered diode parameters.

Finally, the design parameters to fabricate such a Schottky-barrier-diode-based SPP waveguide are proposed in detail. Ultimately, these results can be utilized as a guide to model SPP propagation in Schottky waveguides with added benefits such as simple, power-efficient, and eased integration improving the performance of plasmonic devices.

References

[1] M. Premaratne and G. P. Agrawal, *Light Propagation in Gain Media: Optical Amplifiers*. Cambridge, U.K.: Cambridge Univ. Press, 2011.
[2] D. Sarid and W. Challener, *Modern Introduction to Surface Plasmons: Theory, Mathematica Modeling and Applications*. Cambridge, U.K.: Cambridge Univ. Press, 2010.
[3] S. A. Maier, *Plasmonics: Fundamentals and Applications*. Berlin, Germany: Springer-Verlag, 2007.
[4] M. Born and E. Wolf, *Principles of Optics*. Cambridge, U.K.: Cambridge Univ. Press, 1999.
[5] E. Ozbay, "Plasmonics: Merging photonics and electronics at nanoscale dimensions," *Science*, vol. 311, no. 5758, pp. 189–193, Jan. 2006.
[6] W. L. Barnes, A. Dereux, and T. W. Ebbesen, "Surface plasmon subwavelength optics," *Nature*, vol. 424, no. 6950, pp. 824–830, Aug. 2003.
[7] J. A. Schuller, E. S. Barnard, W. Cai, Y. C. Jun, J. S. White, and M. L. Brongersma, "Plasmonics for extreme light concentration and manipulation," *Nat. Mater.*, vol. 9, no. 3, pp. 193–204, Mar. 2010.
[8] P. L. Stiles, D. J. Dieringer, N. C. Shah, and R. P. V. Duyne, "Surface-enhanced Raman spectroscopy," *Ann. Rev. Anal. Chem.*, vol. 1, pp. 601–626, Mar. 2008.
[9] S. Kawata, Y. Inouye, and P. Verma, "Plasmonics for near-field nano-imaging and superlensing," *Nat. Photon.*, vol. 3, no. 7, pp. 388–394, Jul. 2009.
[10] J. N. Anker, W. P. Hall, O. Lyandres, N. C. Shah, J. Zhao, and R. P. V. Duyne, "Biosensing with plasmonic nanosensors," *Nat. Mater.*, vol. 7, no. 6, pp. 442–453, Jun. 2008.
[11] W. Srituravanich, N. Fang, C. Sun, Q. Luo, and X. Zhang, "Plasmonic nanolithography," *Nano Lett.*, vol. 4, no. 6, pp. 1085–1088, May 2004.
[12] V. E. Ferry, L. A. Sweatlock, D. Pacifici, and H. A. Atwater, "Plasmonic nanostructure design for efficient light coupling into solar cells," *Nano Lett.*, vol. 8, no. 12, pp. 4391–4397, Dec. 2008.
[13] F. J. G. Vidal, L. M. Moreno, and J. B. Pendry, "Surfaces with holes in them: New plasmonic metamaterials," *J. Opt. A, Pure Appl. Opt.*, vol. 7, no. 2, pp. S97–S101, Feb. 2005.
[14] V. M. Shalaev, "Optical negative-index metamaterials," *Nat. Photon.*, vol. 1, no. 1, pp. 41–48, 2007.
[15] S. A. Maier, "Gain-assisted propagation of electromagnetic energy in subwavelength surface plasmon polariton gap waveguides," *Opt. Commun.*, vol. 258, no. 2, pp. 295–299, Feb. 2006.
[16] I. D. Leon and P. Berini, "Amplification of long-range surface plasmons by a dipolar gain medium," *Nat. Photon.*, vol. 4, no. 6, pp. 382–388, Mar. 2010.
[17] I. B. Udagedara, I. D. Rukhlenko, and M. Premaratne, "Complex-ω approach versus complex-$\mathbf{k}$ approach in description of gain-assisted spp propagation along linear chains of metallic nano spheres," *Phys. Rev. B, Condens. Matter*, vol. 83, no. 11, pp. 115451-1–115451-7, Mar. 2011.
[18] D. S. Citrin, "Plasmon-polariton transport in metal-nanoparticle chains embedded in a gain medium," *Opt. Lett.*, vol. 31, no. 1, pp. 98–100, Jan. 2006.
[19] D. Handapangoda, I. D. Rukhlenko, M. Premaratne, and C. Jagadish, "Optimization of gain-assisted waveguiding in metal-dielectric nanowires," *Opt. Lett.*, vol. 35, no. 24, pp. 4190–4192, Dec. 2010.
[20] D. J. Park, S. B. Choi, K. J. Ahn, D. S. Kim, J. H. Kang, Q.-H. Park, M. S. Jeong, and D. K. Ko, "Experimental verification of surface plasmon amplification on a metallic transmission grating," *Phys. Rev. B, Condens. Matter*, vol. 77, no. 11, pp. 115451-1–115455-4, Mar. 2008.
[21] J. Seidel, S. Grafstrom, and L. Eng, "Stimulated emission of surface plasmons at the interface between a silver film and an optically pumped dye solution," *Phys. Rev. Lett.*, vol. 94, no. 17, pp. 177401-1–177401-4, May 2005.
[22] M. C. Gather, K. Meerholz, N. Danz, and K. Leosson, "Net optical gain in a plasmonic waveguide embedded in a fluorescent polymer," *Nat. Photon.*, vol. 4, no. 7, pp. 457–461, Jul. 2010.
[23] J. Grandidier, G. C. Francs, S. Massenot, A. Bouhelier, L. Markey, J. Weeber, C. Finot, and A. Dereux, "Gain-assisted propagation in a plasmonic waveguide at telecom wavelength," *Nano Lett.*, vol. 9, no. 8, pp. 2935–2939, Aug. 2009.
[24] D. Y. Fedyanin, "Toward an electrically pumped spaser," *Opt. Lett.*, vol. 37, no. 3, pp. 404–406, Feb. 2012.
[25] K. Li, X. Li, M. I. Stockman, and D. J. Bergman, "Surface plasmon amplification by stimulated emission in nanolenses," *Phys. Rev. B*, vol. 71, no. 11, pp. 115 409–115 414, Mar. 2005.
[26] M. Ambati, D. A. Genov, R. F. Oulton, and X. Zhang, "Active plasmonics: Surface plasmon interaction with optical emitters," *IEEE J. Sel. Topics Quantum Electron.*, vol. 14, no. 6, pp. 1395–1403, Nov./Dec. 2008.
[27] T. Wijesinghe and M. Premaratne, "Dispersion relation for surface plasmon polaritons on a Schottky junction," *Opt. Exp.*, vol. 20, no. 7, pp. 7151–7164, Mar. 2012.
[28] D. Y. Fedyanin and A. V. Arsenin, "Surface plasmon polariton amplification in metal-semiconductor structures," *Opt. Exp.*, vol. 19, no. 13, pp. 12 524–12 531, Jun. 2011.
[29] M. I. Stockman, "Loss compensation by gain and spasing," *Philos. Trans. Roy. Soc. A, Math., Phys., Eng. Sci.*, vol. 369, no. 1950, pp. 3510–3524, Sep. 2011.
[30] W. Monch, "Metal-semiconductor contacts: Electronic properties," *Surf. Sci.*, vol. 299/300, pp. 928–944, Jan. 1994.
[31] J. Tersoff, "Schottky barriers and semiconductor band structures," *Phys. Rev. B, Condens. Matter*, vol. 32, no. 10, pp. 6968–6971, Nov. 1985.

[32] C. C. Kao and E. M. Conmell, "Surface plasmon dispersion of semiconductors with depletion or accumulation layers," *Phys. Rev. B, Condens. Matter*, vol. 14, no. 6, pp. 2464–2479, Sep. 1976.
[33] S. L. Cunningham, A. A. Maradudin, and R. F. Wallis, "Effect of a charge layer on the surface-plasmon-polariton dispersion curve," *Phys. Rev. B, Condens. Matter*, vol. 10, no. 8, pp. 3342–3355, Oct. 1974.
[34] A. Yariv and R. C. C. Leite, "Dielectric waveguide mode of light propagation in p-n junctions," *Appl. Phys. Lett.*, vol. 2, no. 3, pp. 55–57, Feb. 1963.
[35] R. F. Wallis, J. J. Brion, E. Burstein, and A. Hartstein, "Theory of surface polaritons in semiconductors," in *Proc. 11th Int. Conf. Phys. Semicond.*, 1972, pp. 1448–1456.
[36] J. C. Inkson, "Many-body effects at metal-semiconductor junctions. I. Surface plasmons and the electron-electron screened interaction," *J. Phys. C, Solid State Phys.*, vol. 5, no. 18, pp. 2599–2610, Sep. 1972.
[37] E. Demoulin and F. V. D. Wiele, "Inversion layers at the interface of Schottky diodes," *Solid State Electron.*, vol. 17, no. 8, pp. 825–833, Aug. 1974.
[38] M. A. Green and J. Shewchun, "Minority carrier effects upon small signal and steady-state properties of Schottky diodes," *Solid State Electron.*, vol. 16, no. 10, pp. 1141–1150, Oct. 1973.
[39] H. Guckel, D. C. Thomas, S. V. Iyengar, and A. Demirkol, "Transition region behavior in abrupt forward biased pn junctions," *Solid State Electron.*, vol. 20, no. 7, pp. 647–652, Jul. 1977.
[40] K. W. Boer, *Introduction to Space Charge Effects in Semiconductors*, 1st ed. New York, NY, USA: Springer-Verlag, 2010.
[41] S. M. Sze and K. K. Ng, *Physics of Semiconductor Devices*, 3rd ed. New York, NY, USA: Wiley, 2006.
[42] D. J. Bartelink, "Surface depletion and inversion in semiconductors with arbitrary dopant profiles," *Appl. Phys. Lett.*, vol. 37, no. 2, pp. 220–224, Jul. 1980.
[43] S. S. De and A. K. Ghosh, "Some analysis of potential profiles of forward-biased high low junctions," *J. Appl. Phys.*, vol. 75, no. 5, pp. 2496–2501, Mar. 1994.
[44] R. Seiwatz and M. Green, "Space charge calculations for semiconductors," *J. Appl. Phys.*, vol. 29, no. 7, pp. 1034–1041, Jul. 1958.
[45] C. Goldberg, "Space charge regions in semiconductors," *Solid State Electron.*, vol. 7, no. 8, pp. 593–609, Aug. 1964.
[46] F. V. D. Wiele and E. Demoulin, "Inversion layers in abrupt p-n junctions," *Solid State Electron.*, vol. 13, no. 6, pp. 717–726, Jun. 1970.
[47] J. I. Pankove, *Optical Processes in Semiconductors*, 1st ed. Englewood Cliffs, NJ, USA: Prentice-Hall, 1971.
[48] S. L. Chuang, *Physics of Photonic Devices*, 2nd ed. Chicester, U.K.: Wiley, 2009.
[49] G. Lindfield and J. Penny, *Numerical Methods: Using MATLAB*, 3rd ed. New York, NY, USA: Academic, 2012.
[50] J. R. Hauser and M. A. Littlejohn, "Approximations for accumulation and inversion space charge layers in semiconductors," *Solid State Electron.*, vol. 11, no. 7, pp. 667–674, Jul. 1968.
[51] K. L. Hall, E. R. Thoen, and E. P. Ippen, *Nonlinear Optics in Semiconductors*. Boston, MA, USA: Academic, 1999, pp. 83–155.
[52] T. D. Visser and B. Demeulenaere, "Confinement and modal gain in dielectric waveguides," *J. Lightw. Technol.*, vol. 14, no. 5, pp. 885–887, May 1996.
[53] J. T. Robinson, K. Preston, O. Painter, and M. Lipson, "First-principle derivation of gain in high-index-contrast waveguides," *Opt. Exp.*, vol. 16, no. 21, pp. 16 659–16 669, Oct. 2008.
[54] E. Pop, "Energy dissipation and transport in nanoscale devices," *Nano Res.*, vol. 3, no. 3, pp. 147–169, Mar. 2010.
[55] D. Fedyanin, A. V. Krasavin, A. V. Arsenin, and A. V. Zayats, "Surface plasmon polariton amplification upon electrical injection in highly integrated plasmonic circuits," *Nano Lett.*, vol. 12, no. 5, pp. 2459–2463, May 2012.